CrossMark

Optimal carbon capture and storage contracts using historical CO$_2$ emissions levels

Dashi I. Singham · Wenbo Cai · Joshua A. White

Abstract In an effort to reduce carbon dioxide (CO$_2$) emissions to the atmosphere, carbon capture and storage (CCS) technology has been developed to collect CO$_2$ from emissions generators and store it underground. Recent proposed legislation would limit the volume of emissions generated from power sources, effectively requiring some sources to participate in CCS. Both emissions sources and storage operators require incentives to enter into contracts to capture excess emissions at the source, and transport and store the CO$_2$ underground. As the level of emissions from power plants is stochastic and carryover into future time periods is expensive, we develop a newsvendor model to determine the optimal price and volume of these contracts to maximize the expected profit of the storage operator and encourage the participation of multiple emissions sources. Because the storage operator has a limit on the amount of CO$_2$ that can be injected each month, this limit affects the allocation of the optimal contract amounts between the emitters. The distribution of emissions and relative costs of transportation also influence the optimal policy. In addition to analytical solutions, we present data-driven methods for using correlated emissions data to determine the optimal price and volume of these contracts.

D. I. Singham (✉)
Operations Research Department, Naval Postgraduate School, Monterey, USA
e-mail: dsingham@nps.edu

W. Cai
Mechanical and Industrial Engineering Department, New Jersey Institute of Technology, Newark, USA
e-mail: cai@njit.edu

J. A. White
Atmospheric, Earth and Energy Division, Lawrence Livermore National Laboratory, Livermore, USA
e-mail: jawhite@llnl.gov

1 Introduction

Carbon capture and storage (CCS) is a technology to reduce CO_2 emissions from power plants and other stationary sources of greenhouse gas emissions. At a facility fitted with carbon capture technology, CO_2 is stripped from the emissions stream, compressed, and transported to a storage site. A storage operator then injects the compressed CO_2 into a deep reservoir (typically between 800 to 3000 m depth) where it remains underground indefinitely. The advantage of CCS is that the world could continue to use widespread fossil fuel resources while minimizing climate change impacts. Also, a number of non-power industrial processes (such as cement production) which make a substantial contribution to global CO_2 emissions but do not yet have green alternatives can also participate in CCS. There are currently eight industrial-scale CCS projects operating around the world, with others in the construction or planning stages [14].

In 2013, the U.S. Environmental Protection Agency (EPA) proposed a performance standard for new electric utility generating units that would set a limit on greenhouse gas emissions [9]. The rule would limit CO_2 emissions from new stationary power-generation sources to 1100 lbs/MWh. The most efficient coal power plant designs emit approximately 1800 lbs/MWh, and therefore no new coal power plants could be built without capturing at least a portion of their emissions. The performance standard is based on the efficiency of new natural-gas power plants, which emit far less CO_2 than coal and can meet the 1100 lbs/MWh limit without retrofitting. The proposed rule, when finally implemented, will only apply to newly constructed generating units. In 2014, the EPA released a second plan to cut greenhouse gas emissions from existing power plants through a series of state/federal partnerships. The target for this second "Clean Power Plan" is to cut carbon emissions from the entire power sector by 30 % from 2005 levels by 2030 [10].

Power plants have an incentive to participate in CCS technology to continue generating electricity to meet demand while avoiding penalties associated with the proposed legislation. The plants must have a financial incentive to participate in CCS for the technology to become widespread. Rather than each plant developing and implementing their own storage technology, the plants can capture their CO_2 and outsource the transportation and storage process to avoid building injection wells and hiring internal engineering and operations teams. Storage operators also require a profit incentive to invest in the transportation and storage infrastructure, and there are only certain locations that are suitable for carbon storage. Thus, the storage operator's best course of action is to contract with multiple power plants to transport their CO_2 to the injection site.

The topic of reducing the carbon footprint of a supply chain has recently attracted attention from operations management researchers. Song and Leng [24] obtain the optimal production quantities under three common carbon emissions policies: strict cap on emissions, carbon tax, and cap-and-trade. Cachon [4] derives and compares the optimal retail supply chain designs under three different objectives: minimizing operating costs, minimizing carbon emissions, and minimizing both. Benjaafar et al. [2] also consider how firms' operational decisions need to be adjusted when accounting for carbon emissions under different carbon polices. Caro et al. [6] analyze the effect

of carbon emission allocation rules (offsetting emissions vs. induced investment) on the decisions of the supply chain players.

Specific details on the capture, transportation, and storage components of CCS are included in [15]. The authors comprehensively describe current optimization efforts to minimize costs in energy expansion planning models, and the decision to implement capture technology in fossil-fuel burning power plants. They also discuss multiple objective models that balance minimizing costs and also minimizing CO_2 emissions, and optimization formulations of pipeline networks. A series of papers [17,20,21] focus on the development and improvement of SimCCS, a model that designs the optimal CCS infrastructure that minimizes the costs of capturing, transporting and storing CO_2 underground. Klokk et al. [19] and Kemp and Kasim [18] consider the optimal design of the CCS infrastructure while incorporating enhanced oil recovery (EOR), and thus create a CO_2 value chain to offset the cost associated with building such infrastructure. Optimal investment schedules for a CO_2 value chain with EOR and CO_2 permit options are derived in [13]. Huang et al. [16] formulate an optimization problem to choose injection rates for CO_2 enhanced coal bed methane production. A real options approach is taken to determine the optimal time to invest in capture technology with unknown CCS costs in [22]. Baker et al. [1] analyze the relationships between cost measures of different carbon capture technologies, and conduct a survey of the literature to compare these costs. Our work complements this research by considering the options available to the storage operator, rather than the power producer.

Esposito et al. [11] discuss different types of CCS business models, which include "Self Build and Operate, Joint-Venture Model, and Pay at the Gate." Whereas the existing CCS models focus on the first business model in which utilities own the reservoirs and build and operate their networks of pipelines, our paper provides a framework for the last model (Pay at the Gate) where utilities capture the CO_2 at the power generating sites and pay the storage operator a service fee that includes both the transportation and storage of CO_2. The storage operator owns the pipeline as well as the storage site. The framework thus allows the power plant emissions sources (called 'emitters' henceforth) to participate in CCS while requiring limited internal expertise and staffing, and the storage operator with the appropriate expertise can provide the service to multiple utilities efficiently.

We consider a scenario where a storage operator needs to decide whether to provide service to emitters in the presence of uncertainty in emissions levels and private information of emitter capture costs. Additionally, the storage operator must determine how large to scale his operations by determining the pipeline size and the service price for transporting and storing CO_2. Whereas the volume of a storage reservoir is generally quite large, there is a limit on the injection rate (called 'capacity') into the well. Because emissions levels vary from month to month, we adopt a multi-product newsvendor model with limited capacity to determine the optimal (monthly) contract amounts and service price.

Cai et al. [5] study the optimal contract design in a CCS supply chain, which consists of a carbon emitter and a storage operator. The goal is to optimize the latter's expected profit while inducing the former to participate in CCS. We extend this work by considering a storage operator's optimal contract design when facing multiple carbon emitters with restricted capacity at the storage site, and by using historical data to drive

the optimization. The newsvendor model is used to incorporate the uncertainty in the emissions, an important factor that affects the storage operator's decision on which emitters to serve, what is the volume he can commit to transport, and consequently, what are the sizes of the pipelines to be built. We deliver insight into how to allocate capacity and pipelines to the different emitters and how this differs from the decisions made when analyzing each emitter separately.

We present three models in Sect. 2. In the single-emitter model, the optimal policy that specifies the contract volume and the price is determined for the storage operator dealing with each power plant separately. In the dual-emitter model, the storage operator must allocate contract volumes to two power plants with heterogeneous transportation costs. The optimal policy prescribes both contract volumes and a unified price. For both of these models, we can determine analytically the optimal contract amounts as functions of both the costs associated with each plant. The "N-emitter" model develops heuristics for estimating the optimal solution when there are more than two emitters. We analyze our results by calibrating emissions distributions using historical emissions data from the EPA's Air Markets Program Database [25]. Section 3 displays the numerical results for each model applied to real emissions data. We fit probability density functions to the emissions data and use these density functions to calculate the optimal contract solutions analytically. We also model the correlation between emitters and determine the optimal contracts under dependent emissions numerically using simulation. Section 4 concludes and all proofs are included in the Appendix.

2 Model

We address the problem of a storage operator who needs to decide whether to provide service to power plant emissions sources and how to price the service to achieve an optimal expected profit. Additionally, the storage operator must determine how large to scale his operations by determining the volume of CO_2 to accept from various emitters with uncertain emissions levels. We structure this problem using a newsvendor model, where the product being sold is the service of transporting and storing CO_2, and the price of the service is proportional to the volume of CO_2 transported and stored. It is too expensive to store excess CO_2 from one time period for injection at a later date. Thus, we focus on a single-period newsvendor method to determine the optimal "order quantity" for each period. Because the emissions levels vary at each time period, the demand faced by the storage operator is random. In order to encourage participation, the storage operator designs contracts that guarantee certain pipeline space to transport the captured CO_2 and store it at a selected injection well. Given that there is a maximum injection rate at the site, there must be a limit on the total monthly contracted amount. We thus study the situation where there are multiple emitters, each of whom has a different transportation cost because of their varying distances to the storage site.

2.1 Contract construction and assumptions

The order of events is as follows. The storage operator estimates the distribution of each plant's historical emissions levels from the data, and the distribution of the capture

cost for all emitters. The operator creates a monthly profit function by combining these distributions with the costs of transporting and storing CO_2, and optimizes the profit function to find the monthly contract volume for each emitter and a unit price of CO_2 that is the same for all emitters.

These contracts are then accepted or rejected by each emitter depending on their actual costs of implementing carbon capture technology. That is, the emitter accepts the contract only if the sum of the capture cost and the service price is less than the alternative options available. The emitter may choose another storage operator if the price is too high, or may choose to emit above the proposed legal limit and pay the associated penalty.

For contracts that are accepted, the storage operator builds the pipeline to accommodate the agreed upon volume by the emitter. If one or more emitters reject the contracts, the operator may choose to build larger pipelines for the ones that have accepted the contracts. The emitter has the right, but not the obligation, to have the agreed-upon volume of CO_2 stored each month. The emitter only pays for the actual volume of CO_2 transported in a particular month, not for the entire contract amount. However, if the emitter wishes to transport more CO_2 than the contract amount because of excess emissions in a particular month, the storage operator may choose to accommodate this request by trucking the excess amount of CO_2 to the storage site, so long as there is space available and the service price is higher than the sum of the trucking cost and the injection cost.

We do not model failures in the emissions plant, pipelines, or storage facility. We assume that the recent proposed legislation is applied equally to the power plants we study, though in reality different rules may apply based on the age of the plant. We also require that the total contract amount will be smaller than or equal to the capacity, so that the storage operator will be able to accommodate all emitters as long as each of them captures within their assigned contract volume.

2.2 Model notation

Let K denote the monthly payment of a one-time setup cost for a selected site. It includes the cost of selecting a reservoir and building the injection well. Let Q represent the maximum injection amount for one month; we call this the capacity. Let c be the marginal injection cost for storing CO_2, α_i the marginal monthly cost for pipeline building and maintenance, and β_i the marginal trucking costs for transporting CO_2 from Emitter i. The transportation costs associated with the emitters differ due to their varying distances from the injection site. Because transportation by pipeline is cheaper than trucking, we further assume that $\alpha_i < \beta_i$. Trucking is only used when an emitter wishes to store more than the contract amount and the pipeline cannot accommodate it. We consider the policy where each emitter is given a cap on their emissions quantity, and excess emissions must be stored using CCS to avoid a penalty. Let t denote the cost of an emitter's best alternative option, which can be using another storage operator's service, employing renewable energy, paying the penalty, etc.

Further, let E_i represent the amount of CO_2 over the limit produced by Emitter i and $f_i(\cdot)$ and $F_i(\cdot)$ denote the density and cumulative distribution function of the excess

emissions (E_i) of Emitter i, respectively. We use $F_i^{-1}(\cdot)$ to represent the inverse of the cumulative distribution function of E_i and $\overline{F_i}(E_i) \equiv 1 - F_i(E_i)$. Because each emitter privately observes his capture cost and has an incentive not to disclose it, we consider the capture cost as a random variable, but its distribution is known. Let $g(\cdot)$ and $G(\cdot)$ denote the density and cumulative distribution function of the emitters' capture cost, respectively. Last, our decision variables include p, the unit price the operator charges the emitters for CO_2 stored, and q_i, the contracted amount of CO_2 transported via pipeline from Emitter i, where Emitter i has the right but not the obligation to ship q_i units via the pipeline.

2.3 Newsvendor models for optimal contracts

We apply the newsvendor model to determine the optimal contracts under different settings. We first review the single-emitter model, where the storage operator designs a contract with one emitter. The second, and main model of this paper, is the dual-emitter model, where there are two emitters with different costs and emissions distributions. In the event where emitters wish to deliver more than their contracted amount, the storage operator will check their available capacity and allocate extra space by transportation costs (the emitter who is closer will get priority). There are analytical solutions for the single- and dual-emitter models, which we calibrate using the historical data for E_i. The third model involves eight emitters in Illinois, where all of them have the joint option to contract with a centrally located CCS site.

2.3.1 Single-emitter model

We first consider the scenario where there is only one emitter, Emitter i. The storage operator designs an optimal contract that specifies a unit service price (p_i) and an amount (q_i) he commits to transport via pipeline and subsequently store at the site. This problem is studied in [5], who show that the storage operator's optimization problem is to maximize his expected profit ($E\Pi_i^S$):

$$\textbf{(P1)} \quad E\Pi_i^S(q_i, p_i) = \max_{q_i, p_i}\{G(t - p_i) \cdot E\Pi_i^S(q_i|p_i) \,|\, \text{s.t.}\, q_i \leq Q\},$$

where

$$E\Pi_i^S(q_i|p_i) = -K - \alpha_i \cdot q_i + (p_i - c) \cdot \int_0^Q \overline{F}(E_i)dE_i - \beta_i \cdot \int_{q_i}^Q \overline{F}(E_i)dE_i.$$

Here, superscript S is used to denote decision variables in the single-emitter model. The optimal contract amount for the single-emitter i (q_i^S) is as follows:

$$q_i^S = \min\{q_i^*, Q\}, \quad \text{where } q_i^* = F_i^{-1}\left(1 - \frac{\alpha_i}{\beta_i}\right). \tag{1}$$

Further, the optimal price (p_i^S) solves the following equation:

$$G(t - p_i^S) \cdot \int_0^Q \overline{F}(E_i) dE_i - g(t - p_i^S) \cdot E\Pi_i^S(q_i^S|p_i^S) = 0. \qquad (2)$$

Consider the special case where emissions follows an exponential distribution: $f(E_i) = \gamma e^{-\gamma E_i}, \forall E_i \geq 0$ and $f(E_i) = 0$ otherwise. Then,

$$q_i^S = \min\left\{\frac{1}{\gamma}\ln(\rho), Q\right\}, \quad \text{where } \rho = \frac{\beta_i}{\alpha_i} > 1.$$

We further assume that Emitter i's private capture cost follows a uniform distribution: $g(x) = U[\mu - \delta, \mu + \delta], \mu > \delta > 0$, and that $\ln(\rho)/\gamma < Q$. The optimal service price has a closed form solution (the derivation is provided in Appendix B):

$$p_i^S = \left(t - (\mu - \delta) + K + \frac{\alpha_i}{\gamma}\ln(\rho) + \frac{\beta_i}{\gamma}\left(\frac{1}{\rho} - e^{-\gamma Q}\right)\right.$$
$$\left. + \frac{c}{\gamma}(1 - e^{-\gamma Q})\right) \Big/ \left(1 + \frac{1}{\gamma}(1 - e^{-\gamma Q})\right).$$

Thus, the higher the trucking cost relative to the pipeline cost, the higher the storage operator wants to commit to in the contract, as long as the capacity is not exceeded. Moreover, an increase in the transportation cost, set-up cost or injection cost can drive up the service price.

2.3.2 Dual-emitter model

We now consider the scenario where the storage operator can choose to contract with two emitters, Emitter 1 and 2. Recall that both emitters share the same capture cost distribution function $g(\cdot)$ but each emitter has his own emissions distribution ($f_i, i = 1, 2$) as well as associated transportation costs (α_i via pipeline and β_i via trucking). We calculate α_i and β_i as linearly proportional to the distance between the emitter and the storage operator. Additionally, we assume without loss of generality that Emitter 1 is located further from the operator than Emitter 2, and thus $\alpha_1 > \alpha_2$ and $\beta_1 > \beta_2$. Because these emitters may be owned or operated by the same utility company, we assume that the storage operator offers an "off-the-shelf" service price, that is, he charges the same price to both emitters.

The storage operator has to balance his available capacity against the risk associated with two separate contracts. In the analytical model, we assume that the emissions distributions of the two emitters are independent, and we provide numerical analysis for the situation where the emissions distributions are correlated in Sect. 3. For given contract amounts q_1 and q_2, there are three possible outcomes to consider in determining how much CO_2 from each emitter gets stored: (i) When both plants emit under their contract amounts, the operator stores the entire emissions quantities from both emitters. (ii) When Emitter i produces above the contract amount while Emitter j produces below the contract amount, the operator accepts the entire emissions quantity from Emitter j first and then provides the rest of the available capacity to Emitter i. (iii) When both plants emit above their contract amounts, the operator accepts the

contract quantities from both emitters first. Because the cost of transporting CO_2 from Emitter 1 is more costly, the operator gives priority to Emitter 2 if there is any capacity available after both contracts are fulfilled. Any overage from Emitter 1 is accepted only if there is excess capacity after the entire emissions quantity from Emitter 2 has been stored.

Optimal contract amounts. The storage operator's objective is thus to choose the optimal contract amounts (q_1, q_2) to maximize his expected profit. Let $E\Pi^D(q_1, q_2|p)$ denote the expected profit given a unit service price p. It can be expressed as
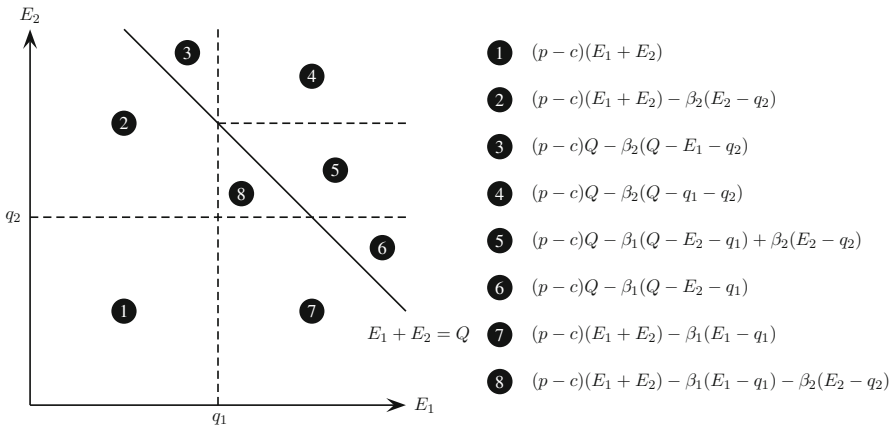
$$
E\Pi^D(q_1, q_2|p) = -K - \alpha_1 \cdot q_1 - \alpha_2 \cdot q_2 + \int_{E_1=0}^{q_1}\int_{E_2=0}^{q_2} (p-c) \cdot (E_1 + E_2) dF_2(E_2) dF_1(E_1)
$$

$$
+ \int_{E_2=0}^{q_2}\int_{E_1=q_1}^{\infty} [(p-c) \cdot \min\{Q, E_1 + E_2\} - \beta_1 \cdot (\min\{Q - E_2, E_1\} - q_1)] dF_1(E_1) dF_2(E_2)
$$

$$
+ \int_{E_1=0}^{q_1}\int_{E_2=q_2}^{\infty} [(p-c) \cdot \min\{Q, E_1 + E_2\} - \beta_2 \cdot (\min\{Q - E_1, E_2\} - q_2)] dF_2(E_2) dF_1(E_1)
$$

$$
+ \int_{E_1=q_1}^{\infty}\int_{E_2=q_2}^{\infty} [(p-c) \cdot \min\{Q, E_1 + E_2\} - \beta_2 \cdot (\min\{E_2, Q - q_1\} - q_2)
$$

$$
- \beta_1 \cdot (\min\{Q - \min\{E_2, Q - q_1\}, E_1\} - q_1)] dF_1(E_1) dF_2(E_2). \tag{3}
$$

Figure 1 illustrates all possible combinations of storage amounts and the associated profit functions in (3). We can then formulate an optimization problem for the storage operator as

$$
\textbf{(P2)} \qquad \max_{q_1, q_2}\{E\Pi^D(q_1, q_2|p) \mid \text{s.t. } q_1 + q_2 \le Q\}.
$$

We use the Lagrangian method to solve (**P2**). The optimal solution to (**P2**) is summarized in Proposition 1 below, and the proof is provided in Appendix A.

Proposition 1 *Let λ denote the Lagrangian multiplier that satisfies the Karush–Kuhn–Tucker conditions (11)–(15) outlined in Appendix A. Let Q^c denote the cutoff value*

①	$(p-c)(E_1 + E_2)$
②	$(p-c)(E_1 + E_2) - \beta_2(E_2 - q_2)$
③	$(p-c)Q - \beta_2(Q - E_1 - q_2)$
④	$(p-c)Q - \beta_2(Q - q_1 - q_2)$
⑤	$(p-c)Q - \beta_1(Q - E_2 - q_1) + \beta_2(E_2 - q_2)$
⑥	$(p-c)Q - \beta_1(Q - E_2 - q_1)$
⑦	$(p-c)(E_1 + E_2) - \beta_1(E_1 - q_1)$
⑧	$(p-c)(E_1 + E_2) - \beta_1(E_1 - q_1) - \beta_2(E_2 - q_2)$

Fig. 1 Profit values in regions of the emissions space for the dual-emitter model

for the capacity that solves

$$F_1^{-1}\left(1 - \frac{\alpha_1}{(\beta_1 - \beta_2) \cdot F_2(Q^c - q_1^D(0)) + \beta_2}\right) + F_2^{-1}\left(1 - \frac{\alpha_2}{\beta_2}\right) = Q^c. \quad (4)$$

When $Q \geq Q^c$, the optimal contract amounts (q_1^D and q_2^D) that maximize the storage operator's expected profit solve the following equations, respectively:

$$F_1(q_1^D) = 1 - \frac{\alpha_1}{(\beta_1 - \beta_2) \cdot F_2(Q - q_1^D) + \beta_2} \quad \text{and} \quad F_2(q_2^D) = 1 - \frac{\alpha_2}{\beta_2}. \quad (5)$$

When $Q < Q^c$, the optimal contract amounts ($q_1^D(\lambda)$ and $q_2^D(\lambda)$) solve the following equations jointly:

$$q_1^D(\lambda) + q_2^D(\lambda) = Q, \text{ where}$$

$$F_1(q_1^D(\lambda)) = 1 - \frac{\alpha_1 + \lambda}{(\beta_1 - \beta_2) \cdot F_2(Q - q_1^D(\lambda)) + \beta_2} \quad \text{and} \quad F_2(q_2^D(\lambda)) = 1 - \frac{\alpha_2 + \lambda}{\beta_2}. \quad (6)$$

We first note that the optimal contract amounts do not depend on p, so we can treat the price optimization separately. Proposition 1 suggests that when the total capacity is sufficiently large ($Q \geq Q^c$), the optimal contract amount for Emitter 2 is the same as that in the single-emitter case, i.e., $q_2^D = q_2^S$. The optimal contract amount for Emitter 1, however, is lower than that when he is considered the sole emissions source, i.e., $q_1^D \leq q_1^S$. When the capacity is restricted ($Q < Q^c$), both optimal contracts are smaller compared to those in the single-emitter cases, that is $q_1^D < q_1^S$ and $q_2^D < q_2^S$.

To provide more intuition for the result, let us consider the special case where the emission quantities for both emitters follow the same exponential distribution with the same rate. The detailed derivation for this special case is provided in Appendix B. When the capacity is sufficiently large, the optimal contract amount for Emitter 1 depends on the site capacity (Q) as well as the difference in the distances between the emitters and the storage site (via $\beta_1 - \beta_2$). Specifically, q_1^D increases and converges to q_1^S as either the site capacity increases or as the difference in distances decreases to zero. When the capacity is restricted, both the optimal contract amounts decrease as the site capacity decreases.

Optimal service price. Recall that the emitter's choice to participate is only based on his private capture cost. He participates only if the sum of the capture cost and the service price is lower than the cost of his next best alternative. Thus, the probability

that an emitter participates is $G(t - p)$. Let $E\Pi^D(q_1^D, q_2^D, p)$ denote the storage operator's expected profit, and we can write his profit optimization problem as

$$E\Pi^D(q_1^D, q_2^D, p) = \max_p \left\{ G^2(t - p) \cdot E\Pi^D(q_1^D, q_2^D|p) \right.$$
$$\left. + G(t - p) \cdot \overline{G}(t - p) \cdot (E\Pi_1^S(q_1^S|p) + E\Pi_2^S(q_2^S|p)) \right\}. \quad (7)$$

The first term in (7) is the storage operator's expected profit when both emitters accept the contract of paying the unit price p. The second term represents the scenario where only one emitter decides to participate in the contract. Because the pipeline is built after the agreement is accepted or rejected, the storage operator can build the pipeline to accommodate the optimal amount computed with the participating emitter as the sole source of emissions. If only Emitter 1 accepts the contract, the storage operator builds a pipeline that can take q_1^S from Emitter 1. Similarly, the storage operator could build a pipeline that can take q_2^S from Emitter 2 if he is the only one who accepts the contract. The following proposition displays the conditions for finding the optimal price.

Proposition 2 *The optimal price (p^D) that maximizes $E\Pi^D(q_1^D, q_2^D, p)$ solves the equation below:*

$$G^2(t - p^D) \cdot \left(\int_0^Q (1 - F_1(E_1) \cdot F_2(Q - E_1)) dE_1 \right) - 2G(t - p^D) \cdot g(t - p^D) \cdot E\Pi^D(q_1^D, q_2^D|p^D)$$

$$+ G(t - p^D) \cdot \overline{G}(t - p^D) \cdot \left(\int_0^Q \overline{F_1}(E_1) dE_1 + \int_0^Q \overline{F_2}(E_2) dE_2 \right)$$

$$+ (2G(t - p^D) - 1) \cdot g(t - p^D) \cdot (E\Pi_1^S(q_1^S|p^D) + E\Pi_2^S(q_2^S|p^D)) = 0. \quad (8)$$

It must also meet the second-order sufficient condition (51) *and the non-negativity conditions* (52).

The proof is in Appendix C. As suggested by Proposition 2, it is difficult to derive the optimal price in a closed form. We thus consider the special case where the emissions follow an exponential distribution ($f(E_i) = \gamma e^{-\gamma E_i}$, $\forall E_i \geq 0$) and the capture cost follows a uniform distribution ($g(x) = U[\mu - \delta, \mu + \delta]$, $\mu > \delta > 0$). We can show that the optimal price p^D decreases in capacity. The derivation is provided in Appendix B. Additionally, we present numerical analysis of the optimal price in Sect. 3 and verify that such a result is robust for more general distributions.

2.3.3 N-emitter model

Finally, we consider the model where the storage operator wishes to determine contracts for more than two emitters. Given a set of contracts q_i and emissions levels E_i from N emitters, we can allocate storage space in a given month using Algorithm 1. Each emitter is guaranteed $\min(E_i, q_i)$ space, and excess space is allocated in order of distance, because closer emitters have lower trucking costs. We can calculate the resulting values of S_i which are the actual stored amounts.

ALGORITHM 1: Allocating space for N-emitter model.

Input: Emissions data for $E_1, \ldots, E_N$, contract amounts q_i, Q, distances from each emitter to CCS
      site.
Output: Volumes of CO_2 stored, $S_1, \ldots, S_N$.
Initialize: $total = \sum_{i=1}^{N} \min(E_i, q_i)$ and $S_i = \min(E_i, q_i)$, and set $i =$index for closest emitter;
while $total < Q$ **do**
   | **if** $E_i > q_i$ **then**
   | | **if** $E_i - q_i < Q - total$ **then**
   | | | $S_i = E_i$;
   | | | $total = total + E_i - q_i$;
   | | **else**
   | | | $S_i = q_i + Q - total$;
   | | | $total = Q$;
   | | **end**
   | **end**
   | Set i to index for next closest emitter;
   | If no more emitters, exit;
end
Output injection amounts $S_1, \ldots, S_N$;

We estimate the expected profit for a series of emissions levels by calculating the associated profit for injected amounts under the different conditions for a given month:

$$\Pi^N(q_1, \ldots, q_N | p) = -K + \sum_{i=1}^{N} ((p - c) \cdot S_i - \beta_i \cdot \mathbf{I}_{S_i > q_i} \cdot (S_i - q_i) - \alpha_i \cdot q_i),$$

(9)

where $\mathbf{I}_x$ is an indicator function for event x. We calculate the expected value of (9) by averaging over the associated values of S_i for the different historical E_i values, and optimize the expected profit numerically to obtain the optimal contract amounts, q_i^N. Rather than using the framework for the expected profit maximized over the price as in (7), we use a simplified expression

$$E \Pi^N \left(q_1^N, \ldots, q_N^N, p \right) = G(t - p) \cdot E \Pi \left(q_1^N, \ldots, q_N^N | p \right)$$

(10)

to model the entire set of contracts as a single acceptance or rejection. To use the same framework as (7) would require enumeration of all the possible acceptance/rejection possibilities and the associated optimal contracts, so we use (10) as an approximation to model the storage operator's expected profit where we model a single probability $G(t - p)$ of all emitters accepting the contract. This heuristic overestimates the risk to the storage operator by treating all the N emitters as having the same capture cost, and hence is a conservative measure of the variation in their expected profit.

3 Experimental results and analysis

Our analysis suggests that the storage operator's decisions on contract amounts and service price is primarily driven by the capacity. By applying our analytical results

Fig. 2 Locations and relative emissions volumes from power plant emitters (*circles*) and possible CCS storage site (*star*)
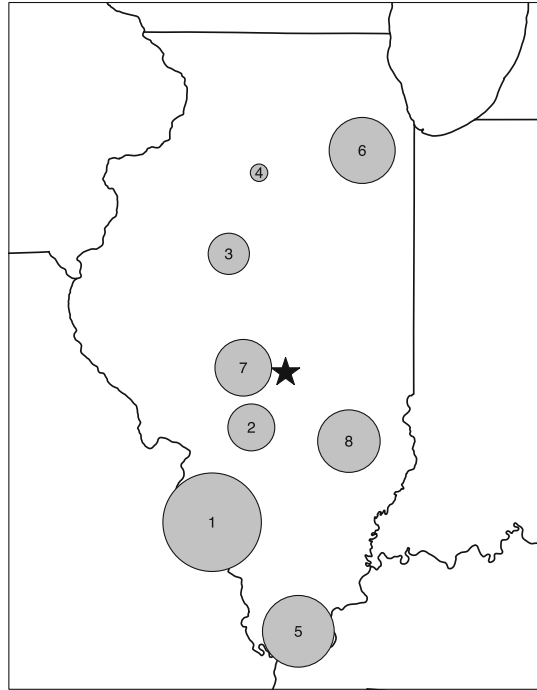
to real emissions data, we arrive at the following results. When capacity is low, the storage operator is more likely to prioritize large emitters or close emitters. The service price may be higher than the price that could be offered separately, but this optimal price decreases as capacity increases. As capacity increases, the proportional contract allocation is larger for the emitter which has larger emissions levels and/or is closer in distance. When the capacity is large, the storage operator offers both emitters the optimal single-emitter contract amounts and lower service prices than they would be offered separately. Additionally, the storage operator's expected profit increases as capacity increases. With a large capacity, both the emitters and the storage operators benefit from joint contracts with multiple emitters.

3.1 Data and methods used

Whereas the proposed EPA rules are only intended for new power plants, we can use emissions data from existing power plants as a proxy data set. Here, we use measured CO_2 emissions data from eight coal-fired power plants in Illinois (Fig. 2). The eight power plants were chosen at random, though they are all larger stations with multiple generating units and significant emissions. They also have a wide geographic distribution through the state, which will impact their associated transportation costs. Illinois was chosen because it is a good target for CCS given the high concentration of coal-fired power in the region. Also, a deep saline aquifer covers much of the state (the Mt. Simon Sandstone, at approximately 2100 m depth) that is widely viewed as

a good storage reservoir for CO_2. The model also contains a hypothetical storage site in the center of the state. The hypothetical site is relatively close to an ongoing CCS demonstration project, the Illinois-Basin Decatur project, which has been injecting CO_2 since 2011 [12].

The data set used here is based on monthly emissions data (Megatonnes (Mt)/month) and gross load (MWh/month) for each of the power plants, covering 13 years of operation from 2000–2012. Based on the proposed EPA cap, we compute the emissions in excess of the cap that must be captured each month to maintain compliance. We also introduce a correction to account for the power consumption associated with the capture process, which leads to a drop in the effective power plant efficiency. A plant with capture technology will typically produce 10–20 % more CO_2 than a plant without capture, and this additional CO_2 must be accounted for [8]. The resulting time histories of excess emissions that must be stored are given in Fig. 3. Coal-fired power plants provide base-load power and typically maintain a fairly constant power output and emissions rate. Nevertheless, rates do vary over time with fluctuating electricity demand. Maintenance shut downs will also lead to occasional drops in emissions. We use a normal distribution for the capture cost with mean \$45/tonne, and a coefficient of variation of one fourth. Cost-of-capture estimates vary widely depending on plant designs and cost assumptions [7,8,23]. The \$45/tonne is a reasonable but conservative value. Some studies project capture costs as low as \$25/tonne. Values for the rest of the model parameters are given in Table 1.

Although the emissions data is not normally distributed (most of the historical time series for the emissions fail the Shapiro–Wilks test for normality), these series are unimodal and the normal distribution provides a tractable method for modeling correlation. Additionally, we find the optimal solutions generated using the fitted normal distributions are similar (with deviations less than 4 %) to those generated using empirical distributions resampled from the data, adding to the robustness of the solutions. In both the dual- and N-emitter cases, correlation between the historical emissions series of the plants may play a role in our results. Using multidimensional normal distributions, we can easily model the dependence between output from emitters, and we use simulated emissions from these dependent distributions to drive a numerical optimization of the optimal price and quantity.

3.2 Single-emitter model

Methods for using data to find robust solutions to the variations of the newsvendor problem exist [3]. For the case where the storage operator only deals with one emitter, we use Eqs. (1) and (2) to find the optimal contract volume and price using fitted normal distributions for each F_i. The optimal contract amounts for each emitter using the single-emitter model are provided in Table 2. Because both the pipeline costs and trucking costs are proportional to the distance between the emitters and the storage site, the ratios of the two costs are the same for all emitters. Thus, the optimal contract amounts are solely driven by the emissions distributions. Plant 1 generates the highest emissions levels. Plant 4 produces the smallest emissions levels, and is relatively far away, and hence has the lowest q_i^S and the highest p_i^S. The optimal prices depend
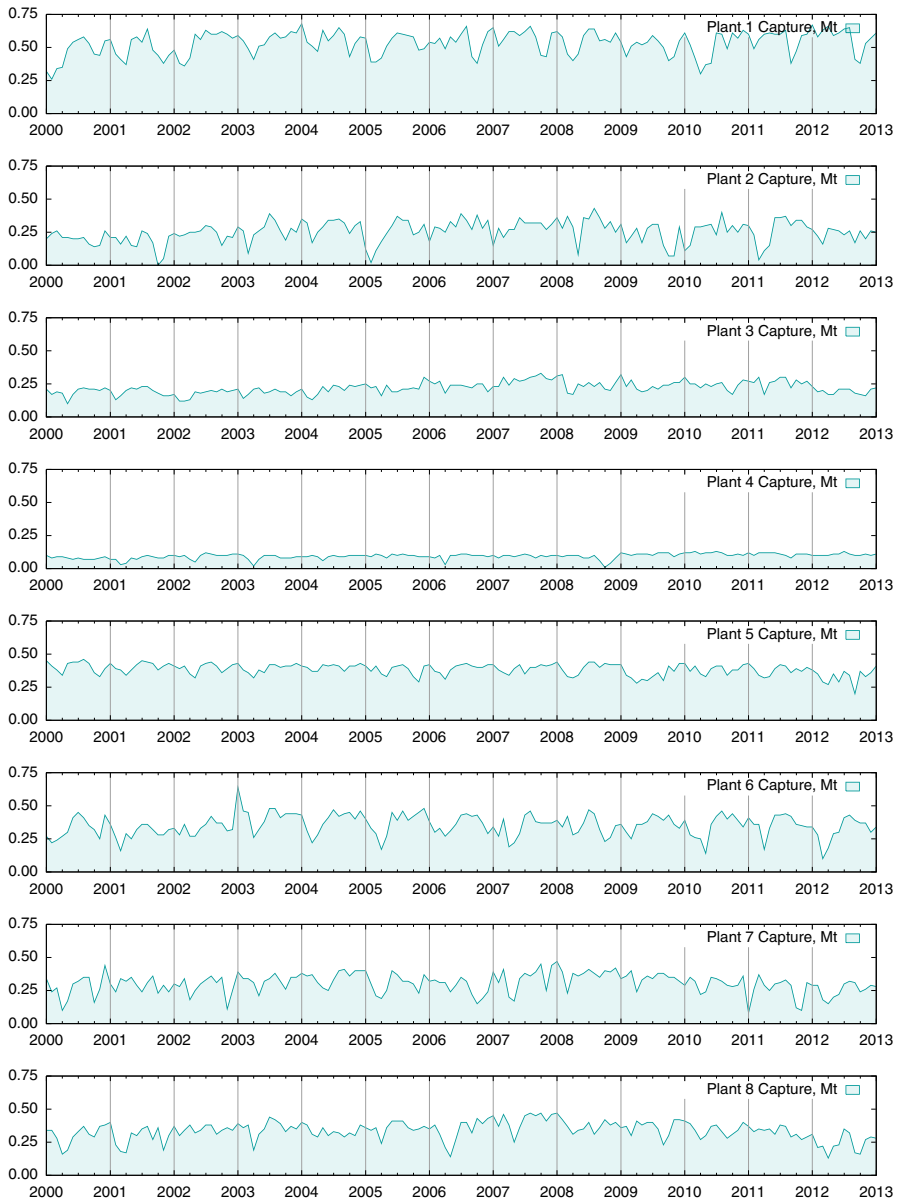
Fig. 3 Capture amount data for the eight emitters

not only on the emissions distributions, but also on the distances between the emitters and the storage site. The expected profit is higher for emitters with larger emissions levels. We use the results from the single-emitter model for comparison with those from dual- and N-emitter models in the next section. This comparison will highlight the effect of relative size and distance on the optimal results.

Table 1 Cost parameter values used in results

Parameter	Value
K (fixed)	$500,000 per month
α (pipeline)	$0.02 per tonne per km
β (trucking)	$0.06 per tonne per km
c (injection)	$7 per tonne
Q (capacity)	1 Mt per month
t (penalty)	$80 per tonne
Distribution of capture cost	$\mathcal{N}(\mu = \$45, \sigma = \$11.25)$ per tonne

Table 2 Optimal monthly contracts for the single-emitter case. The capacity Q is 1 Mt

	q_i^S (Mt)	p_i^S (millions/Mt)	$E\Pi_i^S$ (millions)
Plant 1	0.570	30.987	6.533
Plant 2	0.286	30.554	3.265
Plant 3	0.239	31.204	2.618
Plant 4	0.103	33.280	0.835
Plant 5	0.403	31.945	4.134
Plant 6	0.387	31.957	3.791
Plant 7	0.336	30.135	4.168
Plant 8	0.366	30.680	4.288

3.3 Dual-emitter model

We examine the effects of capacity, distances from the storage sites, emissions levels, and correlation among emissions on the optimal contracts and the storage operator's expected profit.

Effect of capacity. Table 3 provides the optimal quantity allocation between Plants 1 and 2 in the dual-emitter model while varying capacity. In the example, Plant 1 is farther than Plant 2, but Plant 1 has the largest emissions levels. We observe that when Q is small, it is optimal to serve only one emitter. Because Plant 2 is close and $q_2^S = 0.286$, the storage operator only contracts with Plant 2 when $Q \leq 0.20$. As capacity increases, it becomes more profitable to contract with both emitters to diversify the risk if either rejects the contract. The contract amounts for the larger Plant 1 increase much faster than those for the smaller Plant 2. Moreover, the contract amounts converge to the amounts in the single-emitter model. As the capacity increases, the optimal price decreases when both emitters are served, but the storage operator's expected profit increases. This shows that serving both emitters at a single site not only benefits the storage operator but also reduces the cost to the emitters.

Effect of location and correlation of emissions. Table 4 shows the optimal contract amounts for two plants that have comparable emissions levels but large differences in distances in the case where the capacity is restricted ($Q = 0.55$). Plant 5 is located

Table 3 Varying Q for Plant 1 (Emitter 1) and Plant 2 (Emitter 2)

Q	q_1^D (Mt)	q_2^D (Mt)	p^D (millions/Mt)	$E\Pi^D$ (millions)
0.05	0.000	0.050	36.549	0.564
0.10	0.000	0.100	34.808	1.485
0.15	0.000	0.150	34.310	2.392
0.20	0.016	0.184	34.081	3.253
0.25	0.066	0.184	33.865	4.066
0.30	0.116	0.184	33.605	4.820
0.35	0.166	0.184	33.322	5.522
0.40	0.216	0.184	33.038	6.191
0.45	0.266	0.184	32.757	6.831
0.50	0.315	0.185	32.466	7.435
0.55	0.362	0.188	32.148	7.988
0.60	0.405	0.195	31.810	8.482
0.65	0.443	0.207	31.481	8.918
0.70	0.476	0.224	31.191	9.290
0.75	0.506	0.244	30.964	9.593
0.80	0.533	0.267	30.806	9.817
0.85	0.553	0.286	30.709	9.961
0.90	0.562	0.286	30.657	10.044
0.95	0.567	0.286	30.632	10.087
1.00	0.570	0.286	30.622	10.106

Table 4 Optimal results for Plant 5 (Emitter 1) and Plant 7 (Emitter 2) with $Q = 0.55$

	Single emitter	Dual emitter	Dual (dependent)
q (Mt)	0.403, 0.336	0.289, 0.261	0.288, 0.262
p (millions/Mt)	31.94, 30.14	31.95	31.87
$E\Pi$ (millions)	4.13, 4.17	7.52	7.39

farthest from the storage site while Plant 7 is located closest to the site. The first column shows the results from the single-emitter model for each emitter. That is, $q_5^S = 0.403$, $q_7^S = 0.336$. The second column demonstrates the results from the dual-emitter model, i.e., $q_5^D = 0.289$, $q_7^D = 0.261$. Because the capacity is restricted, the storage operator naturally decreases the contract amounts for both emitters when compared to the single-emitter case. Moreover, the reduction rate for Plant 7 is lower, i.e., $(q_5^S - q_5^D)/q_5^S = 28\% > (q_7^S - q_7^D)/q_7^S = 22\%$ despite higher emissions levels than Plant 5. This decision is primarily driven by the fact that Plant 7 is much closer.

The optimal service price ($p^D = \$31.95$) is close to the single-emitter service price for Plant 5 ($p_5^S = \$31.94$). This decision is primarily driven by the fact that the storage capacity is restricted, and thus the storage operator is not worried about the case where only one emitter would accept the contract. If this happens, the storage operator can adjust the quantity carried by the pipeline to the optimal contract amount in the single-emitter case. The unused capacity will be low since both q_5^S and q_7^S are

high enough. He is, however, more concerned about his profit from Plant 5. Because Plant 5 has a higher emissions level and is located far away, the storage operator needs to charge a high price so that he can make a profit comparable to the single-emitter case. Nonetheless, his expected profit is lower than the sum of the expected profits in the single-emitter case because of the restricted capacity, i.e., $E\Pi^D < E\Pi_5^S + E\Pi_7^S$. The final column shows the optimal results calculated via simulation using fitted correlated normal distributions, when correlation between plant emissions is considered. While the optimal contract amounts in the dual-emitter case are not affected by considering correlation, the optimal service price is slightly lower. With positively correlated emissions (the correlation coefficient is +0.30), the variance in total emissions is higher. The storage operator has a stronger incentive to reduce the risk of only one emitter accepting the contract. The expected profit is lower than in the independent case, where the overall emissions stream is expected to be more stable.

For the case where the capacity is large ($Q = 1$), results are displayed in Table 5. Because the capacity is large, the storage operator can offer the contract amounts of the single-emitter case to both emitters, i.e., $q_5^D = q_5^S = 0.403$ and $q_7^D = q_7^S = 0.336$. The optimal service price in the dual-emitter case ($p^D = \$30.89$) is in between those in the single-emitter cases. By setting this price, the storage operator is able to increase the chance that both emitters participate and consequently achieve an expected profit higher than the sum of the expected profits in the single-emitter case, that is, $E\Pi^D > E\Pi_5^S + E\Pi_7^S$. When the correlation in emissions is considered, the optimal contract amounts are not affected while the service price and the storage operator's expected profit both decrease. Similar reasons stated previously apply here as well.

Effect of emissions levels. Table 6 shows the optimal results for Plants 4 and 1. While their distances from the storage sites are comparable, Plant 4 is the smallest emitter while Plant 1 is the largest. We see that in the case of restricted capacity, the reduction rate for Plant 4 is higher, that is, $(q_4^S - q_4^D)/q_4^S = 15\%$ and $(q_1^S - q_1^D)/q_1^S = 10\%$. This suggests that the storage operator should provide a higher reduction rate to the emitter that has lower emissions levels in order to reduce the risk of low emissions quantities from both emitters. Table 7 shows the optimal results for Plants 5 and 6. These two emitters also have comparable distances from the storage sites, but Plant 5

Table 5 Optimal results for Plant 5 (farthest) and Plant 7 (closest) with $Q = 1$

	Single emitter	Dual emitter	Dual (dependent)
q (Mt)	0.403, 0.336	0.403, 0.336	0.403, 0.336
p (millions/Mt)	31.94, 30.14	30.89	30.76
$E\Pi$ (millions)	4.13, 4.17	8.68	8.48

Table 6 Optimal results for Plant 4 (Emitter 1) and Plant 1 (Emitter 2) with $Q = 0.6$

	Single emitter	Dual emitter	Dual (dependent)
q (Mt)	0.103, 0.570	0.087, 0.513	0.087, 0.513
p (millions/Mt)	33.28, 30.95	31.25	31.09
$E\Pi$ (millions)	0.835, 6.43	7.40	7.17

**Table 7** Optimal results for Plant 5 (Emitter 1) and Plant 6 (Emitter 2) with $Q = 0.55$

	Single emitter	Dual emitter	Dual (dependent)
q (Mt)	0.403, 0.387	0.310, 0.240	0.310, 0.240
p (millions/Mt)	31.94, 31.96	32.98	32.78
$E\Pi$ (millions)	4.13, 3.79	7.47	6.97

has a higher emission level, and thus the contract amount reduction is higher for the smaller emitter (Plant 6), i.e., $(q_5^S - q_5^D)/q_5^S = 23\% < (q_6^S - q_6^D)/q_6^S = 38\%$.

In Table 6, the optimal service price in the dual-emitter case ($p^D = \$31.25$) is in between those of the single-emitter cases ($p_4^S = \$33.28$ and $p_1^S = \$30.95$). Moreover, it is closer to the single-emitter service price for Plant 1. This is because setting a service price too high will increase the risk of Plant 1 not participating, which will lead to the capacity being largely unused due to small emissions levels of Plant 4. Due to comparable emissions levels between Plants 5 and 6, the service price in the dual-emitter case ($p^D = \$32.98$) is higher than both prices in the single-emitter cases ($p_5^S = \$31.94$ and $p_6^S = \$31.96$).

3.4 N-emitter model

For the N-emitter case, Fig. 4 shows the optimal contract amounts as the capacity at the storage site increases from 0.4 to 3 Mt. When Q is very small, the storage operator allocates positive contract amounts to all plants except for Plant 5, the one located farthest from the storage site. As the capacity increases, we see greater rates of increase in the contract amounts of Plants 2, 7 and 8 than those of Plants 1, 3, 4 and 6. This is primarily because Plants 2, 7 and 8 are closer than the others. When the capacity is near 1 Mt, there is a sharp increase in the contract amount of Plants 1 and 8 and a sizable decrease in Plant 4, while the others continue to grow steadily. This is
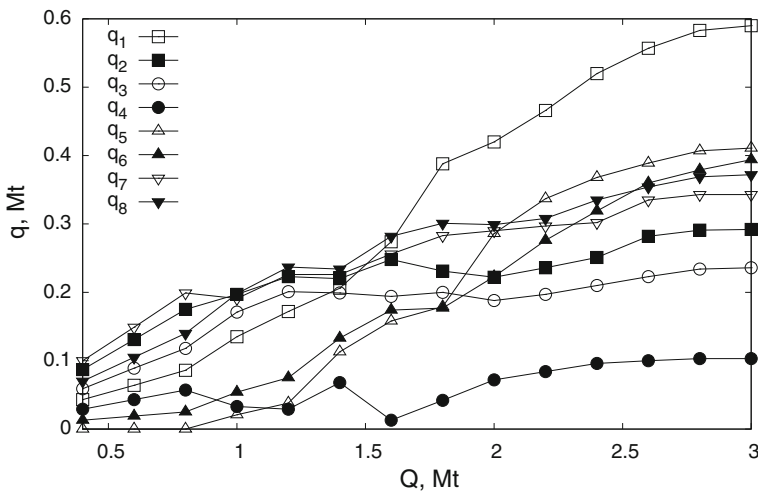
Fig. 4 Optimal contract amounts for the N-emitter model

Table 8 Absolute differences using heuristic solution, compared to Table 3 for Plant 1 and Plant 2 while varying Q

Q	$\hat{q}_1 - q_1^*$ (Mt)	$\hat{q}_2 - q_2^*$ (Mt)	$\hat{p} - p^*$ (millions/per tonne)	$E[\hat{\Pi}] - E[\Pi]$ (millions)
0.05	0.006	−0.006	−2.719	−0.150
0.10	0.019	−0.019	−3.047	−0.379
0.15	0.042	−0.042	−3.122	−0.599
0.20	0.058	−0.058	−3.135	−0.782
0.25	0.046	−0.046	−3.050	−0.922
0.30	0.049	−0.049	−2.854	−1.014
0.35	0.042	−0.042	−2.629	−1.048
0.40	0.049	−0.049	−2.372	−1.059
0.45	0.027	−0.027	−2.140	−1.026
0.50	0.017	−0.017	−1.876	−0.973
0.55	0.017	−0.017	−1.581	−0.892
0.60	0.014	−0.014	−1.256	−0.779
0.65	0.004	−0.004	−0.940	−0.654
0.70	0.006	−0.006	−0.650	−0.520
0.75	0.023	−0.023	−0.413	−0.400
0.80	0.017	−0.017	−0.257	−0.247
0.85	0.005	0.006	−0.155	−0.118
0.90	0.012	0.007	−0.088	−0.028
0.95	0.017	0.006	−0.053	0.023
1.00	0.020	0.007	−0.037	0.037

because Plant 4 is not only located far away from the storage site, but it also has very small emissions levels. The storage operator is better off keeping a higher allocation for larger emitters, such as Plants 1 and 8.

This non-monotonicity appears again as Q is near 1.5 Mt; both the contract amounts of Plants 2 and 4 (the smallest two emitters) decrease as significant increases occur in the contract amounts of Plants 1, 5 and 6. This is primarily driven by emissions levels as they are the biggest emitters. As the capacity becomes higher, the optimal contract amounts converge to those in the single-emitter case.

To assess the quality of our heuristic, we compare it to the optimal solution using the dual-emitter model used in Table 3 to show the effect of changing the capacity Q. Table 8 shows the absolute differences in the optimal results using our heuristic code (with outputs $\hat{q}$, $\hat{p}$, and $E[\hat{\Pi}]$) compared to the dual-emitter optimal results. The heuristic uses historical data to form an expected profit function given emissions that were realized, while the numerical results for the dual-emitter mode fit a normal distribution to the data. In addition to the limitations of relying on numerical optimization without knowledge of the objective function space, the heuristic faces the limitation of assuming all emitters either accept or reject the contracts together.

We chose to use absolute differences to better differentiate units across columns of the table. Table 8 reveals that as the capacity increases and the problem becomes unconstrained, the heuristic solution approaches the optimal solution. Contract alloca-

tions are comparable generally, but the heuristic favors allocating more to Plant 1 than Plant 2 relative to the dual-emitter optimal solution. The price is significantly lower for small capacity sizes, reflecting the desire to induce participation given that the storage operator faces additional risk, as the emitters must either both reject or both accept the contract under the heuristic. As a result, the expected profit is significantly lower in the small capacity cases. We expect this heuristic to provide lower expected profits than the true optimal as the dimensionality of the problem increases in the number of emitters. However, we also note that there is error associated in fitting distributions to data that affects the dual-emitter optimal solution that is not accounted for in the numerical results.

4 Conclusion

We study the problem of designing optimal contracts between a storage operator and multiple CO_2 emitters. We model it as a newsvendor problem, where demands (emissions levels) are uncertain but their distributions are estimated by historical emissions data. The storage operator has a limited capacity for CO_2 that can be injected each month, and this limit may be less than the sum of the optimal amounts that would be injected if each plant was considered separately. There are upfront costs of building a pipeline to support the contract, and higher per unit costs to truck excess CO_2 above the contract level. We also model the likelihood that the emitter will accept the contract based on their costs of capturing CO_2. We find an optimal solution for the case where there are two emitters, and develop a heuristic to solve the case where there are N emitters. The solution provides the storage operator with the optimal contract volumes and a common service price that he should offer to the emitters.

We explore the effect of various governing parameters on the optimal contract amounts. When the capacity is restricted, the storage operator adjusts contract amounts downward from the single-emitter case, and we describe the factors that influence the corresponding allocations. As capacity increases, the optimal contract amounts approach those that would be offered in the single-emitter case. When capacity is large, the expected profit is higher than the sum of the profits for each emitter in the single-emitter case because of the added diversification from multiple emitters. The relative costs of transportation for each emitter, which we take to be functions of distances from the storage site, also affect the optimal contract amounts. Additionally the distribution of the emissions drives the capacity allocations, particularly the overall scale of emissions levels. We demonstrate that if the storage operator has a large capacity, contracting with multiple emitters reduces risk associated with emissions uncertainty, and consequently reduces the price of the service while increasing the expected profit.

Appendix A: Proof of Proposition 1

Proof of Proposition 1 To solve the constrained optimization problem (**P2**), we apply the Lagrangian method. Let $\mathcal{L}(q_1, q_2; \lambda) = E\Pi^D(q_1, q_2|p) - \lambda \cdot (q_1 + q_2 - Q)$. The Karush–Kuhn–Tucker conditions for the optimal solution are:

$$\frac{\partial \mathcal{L}(q_1, q_2; \lambda)}{\partial q_1} = \frac{\partial E\Pi^D(q_1, q_2|p)}{\partial q_1} - \lambda = 0 \tag{11}$$

$$\frac{\partial \mathcal{L}(q_1, q_2; \lambda)}{\partial q_2} = \frac{\partial E\Pi^D(q_1, q_2|p)}{\partial q_2} - \lambda = 0 \tag{12}$$

$$\lambda \cdot (q_1 + q_2 - Q) = 0 \tag{13}$$

$$q_1 + q_2 - Q \leq 0 \tag{14}$$

$$q_1, q_2, \lambda \geq 0 \tag{15}$$

To compute $\frac{\partial E\Pi^D(q_1, q_2|p)}{\partial q_1}$ and $\frac{\partial E\Pi^D(q_1, q_2|p)}{\partial q_2}$, we first rewrite the profit function according to Fig. 1 as

$$E\Pi^D(q_1, q_2|p) = -K - \alpha_1 \cdot q_1 - \alpha_2 \cdot q_2 + \int_{E_1=0}^{q_1} \int_{E_2=0}^{q_2} (p-c) \cdot (E_1+E_2) dF_2(E_2) dF_1(E_1)$$

$$+ \int_{E_2=0}^{q_2} \int_{E_1=q_1}^{Q-E_2} (p-c) \cdot (E_1+E_2) - \beta_1(E_1-q_1) dF_1(E_1) dF_2(E_2)$$

$$+ \int_{E_2=0}^{q_2} \int_{E_1=Q-E_2}^{\infty} (p-c) \cdot Q - \beta_1(Q-E_2-q_1) dF_1(E_1) dF_2(E_2)$$

$$+ \int_{E_1=0}^{q_1} \int_{E_2=q_2}^{Q-E_1} (p-c) \cdot (E_1+E_2) - \beta_2(E_2-q_2) dF_2(E_2) dF_1(E_1)$$

$$+ \int_{E_1=0}^{q_1} \int_{E_2=Q-E_1}^{\infty} (p-c) \cdot Q - \beta_2(Q-E_1-q_2) dF_2(E_2) dF_1(E_1)$$

$$+ \int_{E_2=q_2}^{Q-q_1} \int_{E_1=q_1}^{Q-E_2} (p-c) \cdot (E_1+E_2) - \beta_1(E_1-q_1) - \beta_2(E_2-q_2) dF_1(E_1) dF_2(E_2)$$

$$+ \int_{E_2=q_2}^{Q-q_1} \int_{E_1=Q-E_2}^{\infty} (p-c) \cdot Q - \beta_1(Q-E_2-q_1) - \beta_2(E_2-q_2) dF_1(E_1) dF_2(E_2)$$

$$+ \int_{E_1=q_1}^{\infty} \int_{E_2=Q-q_1}^{\infty} (p-c) \cdot Q - \beta_2(Q-q_1-q_2) dF_2(E_2) dF_1(E_1). \tag{16}$$

$$\frac{\partial E\Pi^D(q_1, q_2|p)}{\partial q_1} = -\alpha_1 + f_1(q_1) \int_{E_2=0}^{q_2} (p-c) \cdot (q_1+E_2) dF_2(E_2)$$

$$+ \int_{E_1=q_1}^{Q-E_2} \left(\int_{E_2=0}^{q_2} \beta_1 dF_2(E_2) \right) dF_1(E_1)$$

$$- f_1(q_1) \int_{E_2=0}^{q_2} (p-c) \cdot (q_1+E_2) dF_2(E_2)$$

$$+ \int_{E_1=Q-E_2}^{\infty} \left(\int_{E_2=0}^{q_2} \beta_1 dF_2(E_2) \right) dF_1(E_1)$$

$$+ f_1(q_1) \int_{E_2=q_2}^{Q-q_1} (p-c) \cdot (q_1+E_2) - \beta_2(E_2-q_2) dF_2(E_2)$$

$$+ f_1(q_1) \int_{E_2=Q-q_1}^{\infty} (p-c)Q - \beta_2(Q-q_1-q_2) dF_2(E_2)$$

$$+ \int_{E_2=q_2}^{Q-q_1} \left(\int_{E_1=q_1}^{Q-E_2} \beta_1 dF_1(E_1) - f_1(q_1) \cdot [(p-c) \cdot (q_1+E_2) - \beta_2(E_2-q_2)] \right) dF_2(E_2)$$

$$+ \int_{E_2=q_2}^{Q-q_1} \left(\int_{E_1=Q-E_2}^{\infty} \beta_1 dF_1(E_1) \right) dF_2(E_2)$$

$$+ f_2(Q - q_1) \int_{E_1=q_1}^{\infty} (p - c)Q - \beta_2(Q - q_1 - q_2)dF_1(E_1)$$

$$+ \int_{E_1=q_1}^{\infty} \left(\int_{E_2=Q-q_1}^{\infty} \beta_2 dF_2(E_2) - f_2(Q - q_1) \cdot [(p-c) \cdot Q - \beta_2(Q - q_1 - q_2)] \right) dF_1(E_1)$$

$$- f_1(q_1) \int_{E_2=Q-q_1}^{\infty} (p - c)Q - \beta_2(Q - q_1 - q_2)dF_2(E_2) \tag{17}$$

$$\frac{\partial E \Pi^D(q_1, q_2 | p)}{\partial q_1} = -\alpha_1 + \int_{E_1=q_1}^{\infty} \int_{E_2=0}^{q_2} \beta_1 dF_2(E_2)dF_1(E_1)$$

$$+ \int_{E_2=q_2}^{Q-q_1} \int_{E_1=q_1}^{\infty} \beta_1 dF_1(E_1)dF_2(E_2)$$

$$+ \int_{E_1=q_1}^{\infty} \int_{E_2=Q-q_1}^{\infty} \beta_2 dF_2(E_2)dF_1(E_1) \tag{18}$$

$$\frac{\partial E \Pi^D(q_1, q_2 | p)}{\partial q_1}$$

$$= -\alpha_1 + \int_{E_1=q_1}^{\infty} \left(\int_{E_2=0}^{Q-q_1} \beta_1 dF_2(E_2) + \int_{E_2=Q-q_1}^{\infty} \beta_2 dF_2(E_2) \right) dF_1(E_1) \tag{19}$$

$$\frac{\partial E \Pi^D(q_1, q_2 | p)}{\partial q_1} = -\alpha_1 + \overline{F_1}(q_1) \left(\beta_1 F_2(Q - q_1) + \beta_2 \overline{F_2}(Q - q_1) \right) \tag{20}$$

Thus, (11) becomes $-\alpha_1 + \overline{F_1}(q_1)(\beta_1 F_2(Q - q_1) + \beta_2 \overline{F_2}(Q - q_1)) - \lambda = 0$, i.e., $q_1^D(\lambda) = F_1^{-1}(1 - \frac{\alpha_1 + \lambda}{(\beta_1 - \beta_2) \cdot F_2(Q - q_1^D(\lambda)) + \beta_2})$.

Also, $\mathcal{L}^2_{q_1 q_2} \equiv \frac{\partial^2 \mathcal{L}(q_1, q_2; \lambda)}{\partial q_1 \partial q_2} = 0$ and $\mathcal{L}^2_{q_1^2} \equiv \frac{\partial^2 \mathcal{L}(q_1, q_2; \lambda)}{\partial q_1^2} = -f_1(q_1)$ $(\beta_1 F_2(Q - q_1) + \beta_2 \overline{F_2}(Q - q_1)) - \overline{F_1}(q_1) \cdot f_2(Q - q_1) \cdot (\beta_1 - \beta_2) < 0$.

$$\frac{\partial E \Pi^D(q_1, q_2 | p)}{\partial q_2} = -\alpha_2 + f_2(q_2) \int_{E_1=0}^{q_1} (p - c)(E_1 + q_2)dF_1(E_1)$$

$$+ f_2(q_2) \int_{E_1=q_1}^{Q-q_2} (p - c) \cdot (E_1 + q_2) - \beta_1(E_1 - q_1)dF_1(E_1)$$

$$+ f_2(q_2) \int_{E_1=Q-q_2}^{\infty} (p - c) \cdot Q - \beta_1(Q - q_1 - q_2)dF_1(E_1)$$

$$+ \int_{E_1=0}^{q_1} \left(\int_{E_2=Q-E_1}^{\infty} \beta_2 dF_2(E_2) \right) dF_1(E_1)$$

$$+ \int_{E_1=0}^{q_1} \left(\int_{E_2=q_2}^{Q-E_1} \beta_2 dF_2(E_2) - f_2(q_2) \cdot (p - c) \cdot (E_1 + q_2) \right) dF_1(E_1)$$

$$+ \int_{E_2=q_2}^{Q-q_1} \left(\int_{E_1=q_1}^{Q-E_2} \beta_2 dF_1(E_1) \right) dF_2(E_2)$$

$$- f_2(q_2) \cdot \int_{E_1=q_1}^{Q-q_2} (p-c) \cdot (E_1 + q_2) - \beta_1(E_1 - q_1) dF_1(E_1)$$

$$+ \int_{E_2=q_2}^{Q-q_1} \left(\int_{E_1=Q-E_2}^{\infty} \beta_2 dF_1(E_1) \right) dF_2(E_2)$$

$$- f_2(q_2) \cdot \int_{E_1=Q-q_2}^{\infty} (p-c)Q - \beta_1(Q - q_1 - q_2) dF_1(E_1)$$

$$+ \int_{E_1=q_1}^{\infty} \left(\int_{E_2=Q-q_1}^{\infty} \beta_2 dF_2(E_2) \right) dF_1(E_1) \tag{21}$$

$$\frac{\partial E\Pi^D(q_1, q_2|p)}{\partial q_2} = -\alpha_2 + \int_{E_1=0}^{q_1} \int_{E_2=q_2}^{Q-E_1} \beta_2 dF_2(E_2) dF_1(E_1)$$

$$+ \int_{E_1=0}^{q_1} \int_{E_2=Q-E_1}^{\infty} \beta_2 dF_2(E_2) dF_1(E_1)$$

$$+ \int_{E_2=q_2}^{Q-q_1} \int_{E_1=q_1}^{Q-E_2} \beta_2 dF_1(E_1) dF_2(E_2)$$

$$+ \int_{E_2=q_2}^{Q-q_1} \int_{E_1=Q-E_2}^{\infty} \beta_2 dF_1(E_1) dF_2(E_2)$$

$$+ \int_{E_1=q_1}^{\infty} \int_{E_2=Q-q_1}^{\infty} \beta_2 dF_2(E_2) dF_1(E_1) \tag{22}$$

$$\frac{\partial E\Pi^D(q_1, q_2|p)}{\partial q_2} = -\alpha_2 + \int_{E_1=0}^{q_1} \int_{E_2=q_2}^{\infty} \beta_2 dF_2(E_2) dF_1(E_1)$$

$$+ \int_{E_1=q_1}^{\infty} \int_{E_2=q_2}^{\infty} \beta_2 dF_2(E_2) dF_1(E_1)$$

$$= -\alpha_2 + \beta_2 \overline{F_2}(q_2) \tag{23}$$

Thus, (12) becomes $-\alpha_2 + \beta_2 \overline{F_2}(q_2) - \lambda = 0$, i.e., $q_2^D(\lambda) = F_2^{-1}(1 - \frac{\alpha_2 + \lambda}{\beta_2})$.
Also, $\mathcal{L}_{q_2q_1}^2 \equiv \frac{\partial^2 \mathcal{L}(q_1, q_2; \lambda)}{\partial q_2 \partial q_1} = 0$ and $\mathcal{L}_{q_2^2}^2 \equiv \frac{\partial^2 \mathcal{L}(q_1, q_2; \lambda)}{\partial q_2^2} = \frac{\partial^2 E\Pi^D(q_1, q_2|p)}{\partial q_2^2} = -f_2(q_2) \cdot \beta_2 < 0$.
We first compute Q^c as the solution for Q in $q_1^D(0) + q_2^D(0) = Q$, i.e.,

$$F_1^{-1} \left(1 - \frac{\alpha_1}{(\beta_1 - \beta_2) \cdot F_2(Q^c - q_1^D(0)) + \beta_2} \right) + F_2^{-1} \left(1 - \frac{\alpha_2}{\beta_2} \right) = Q^c.$$

To find the optimal solution, we consider two cases.

Case 1: $Q \geq Q^c$, then $q_1^D(0) + q_2^D(0) \leq Q$ is satisfied with $\lambda = 0$. The optimal contract amounts solve the following equations: $F_1(q_1^D) = 1 - \frac{\alpha_1}{(\beta_1 - \beta_2) \cdot F_2(Q - q_1^D) + \beta_2}$ and $F_2(q_2^D) = 1 - \frac{\alpha_2}{\beta_2}$.

Case 2: $Q < Q^c$, $q_1^D + q_2^D \leq Q$ is violated. We thus need to solve for λ using $q_1^D(\lambda) + q_2^D(\lambda) = Q$. Because $\mathcal{L}_{q_1^2}^2 < 0$ and $\mathcal{L}_{q_1^2}^2 \mathcal{L}_{q_2^2}^2 - \mathcal{L}_{q_1 q_2}^2 \mathcal{L}_{q_2 q_1}^2 > 0$, $\mathcal{L}$ is concave. Thus, the optimal solution satisfies all KKT conditions and meets the second-order sufficient conditions as well.   □

Appendix B: Derivation of the results for the special case

Single-emitter case. First, we compute q_i^*.

$$\overline{F_i}(q_i^*) = e^{-\gamma q_i^*} = \frac{\alpha_2}{\beta_2} \quad \Rightarrow q_i^* = \frac{1}{\gamma} \ln\left(\frac{\beta_i}{\alpha_i}\right). \tag{24}$$

$$\text{Equation (2)} \Rightarrow E\Pi(q_i^*|p_i) = -K - \frac{\alpha_i}{\gamma} \ln(\rho) - \frac{\beta_i}{\gamma}\left(\frac{1}{\rho} - e^{-\gamma Q}\right)$$
$$+ \frac{p - c}{\gamma}(1 - e^{-\gamma Q}), \tag{25}$$

$$\frac{t - p_i^S - (\mu - \delta)}{2\delta}\left(1 + \frac{1}{\gamma}(1 - e^{-\gamma Q})\right) = \frac{1}{2\delta} E\Pi(q_i^*|p_i)$$
$$\Rightarrow p_i^S = \left(t - (\mu - \delta) + K + \frac{\alpha_i}{\gamma}\ln(\rho) + \frac{\beta_i}{\gamma}\left(\frac{1}{\rho} - e^{-\gamma Q}\right) + \frac{c}{\gamma}(1 - e^{-\gamma Q})\right) \Big/$$
$$\left(1 + \frac{1}{\gamma}(1 - e^{-\gamma Q})\right). \tag{26}$$

Dual-emitter case. First, we compute q_1^D, q_2^D, and $E\Pi^D(q_1^D, q_2^D|p)$.

$$\overline{F_2}(q_2) = e^{-\gamma q_2} = \frac{\alpha_2}{\beta_2} \quad \Rightarrow q_2^D = \frac{1}{\gamma} \ln\left(\frac{\beta_2}{\alpha_2}\right). \tag{27}$$

$$\overline{F_1}(q_1) = e^{-\gamma q_1} = \frac{\alpha_1}{(1 - e^{-\gamma(Q - q_1)})(\beta_1 - \beta_2) + \beta_2} \Rightarrow$$
$$q_1^D = \frac{1}{\gamma} \ln\left(\frac{\beta_1}{\alpha_1 + e^{-\gamma Q}(\beta_1 - \beta_2)}\right). \tag{28}$$

$$\text{Let } \overline{\rho} = \frac{\beta_1}{\alpha_1 + e^{-\gamma Q}(\beta_1 - \beta_2)},$$
$$E\Pi^D(q_1^D, q_2^D|p) = -K - \frac{\alpha_1}{\gamma} \ln(\overline{\rho}) - \frac{\alpha_2}{\gamma} \ln(\rho)$$
$$+ (p - c)\left(\frac{2}{\gamma}(1 - e^{-\gamma Q}) - Qe^{-\gamma Q}\right)$$

$$- \beta_2 \left(\frac{1}{\gamma} \left(\frac{1}{\rho} - e^{-\gamma Q} \right) - e^{-\gamma Q} q_1^D \right)$$

$$- \beta_1 \left(\frac{1}{\gamma} \left(\frac{1}{\rho} - e^{-\gamma Q} \right) - e^{-\gamma Q} (Q - q_1^D) \right). \tag{29}$$

Next, we compute Q^c and λ.

$$Q^c = q_1^D + q_2^D = \frac{1}{\gamma} \ln \left(\frac{(\alpha_1 + e^{-\gamma Q^c}(\beta_1 - \beta_2))\alpha_2}{\beta_1 \beta_2} \right)$$

$$\Rightarrow Q^c = \frac{1}{\gamma} \ln \left(\frac{\beta_1 \beta_2 - (\beta_1 - \beta_2)\alpha_2}{\alpha_1 \alpha_2} \right). \tag{30}$$

$$e^{-\gamma q_1} = \frac{\alpha_1 + \lambda}{(1 - e^{-\gamma(Q - q_1)})(\beta_1 - \beta_2) + \beta_2}$$

$$\Rightarrow q_1^D(\lambda) = \frac{1}{\gamma} \ln \left(\frac{\beta_1}{\alpha_1 + \lambda + e^{-\gamma Q}(\beta_1 - \beta_2)} \right), \tag{31}$$

$$e^{-\gamma q_2} = \frac{\alpha_2 + \lambda}{\beta_2} \quad \Rightarrow q_2^D(\lambda) = \frac{1}{\gamma} \ln \left(\frac{\beta_2}{\alpha_2 + \lambda} \right). \tag{32}$$

$$q_1^D(\lambda) + q_2^D(\lambda) = Q \Rightarrow (\alpha_1 + \lambda + (\beta_1 - \beta_2)e^{-\gamma Q})(\alpha_2 + \lambda) - \beta_1 \beta_2 e^{-\gamma Q} = 0$$

$$\Rightarrow \lambda = \frac{1}{2} \sqrt{(\alpha_1 - \alpha_2 + e^{-\gamma Q}(\beta_1 - \beta_2))^2 + 4\beta_1 \beta_2 e^{-\gamma Q}}$$

$$- \frac{1}{2}(\alpha_1 + \alpha_2 + e^{-\gamma Q}(\beta_1 - \beta_2)). \tag{33}$$

We also need to show that $\lambda > 0$ as long as $\beta_2 > \alpha_1$, and $\frac{\partial \lambda}{\partial Q} < 0$. $Q < Q^c \Rightarrow$ $e^{-\gamma Q} > e^{-\gamma Q^c} = \frac{\beta_1 \beta_2 - (\beta_1 - \beta_2)\alpha_2}{\alpha_1 \alpha_2}$. Thus,

$$(\alpha_1 - \alpha_2 + e^{-\gamma Q}(\beta_1 - \beta_2))^2 + 4\beta_1 \beta_2 e^{-\gamma Q} - (\alpha_1 + \alpha_2 + e^{-\gamma Q}(\beta_1 - \beta_2))^2$$

$$= 4(\beta_1 \beta_2 e^{-\gamma Q} - \alpha_1 \alpha_2 - \alpha_2 e^{-\gamma Q}(\beta_1 - \beta_2))$$

$$= 4(e^{-\gamma Q} \beta_1(\beta_2 - \alpha_2) + \alpha_2(e^{-\gamma Q}\beta_2 - \alpha_1))$$

$$> e^{-\gamma Q} \beta_1(\beta_2 - \alpha_2) + \alpha_2 \left(\frac{\beta_1 \beta_2 - (\beta_1 - \beta_2)\alpha_2}{\alpha_1 \alpha_2} \beta_2 - \alpha_1 \right)$$

$$= e^{-\gamma Q} \beta_1(\beta_2 - \alpha_2) + \frac{1}{\alpha_1}(\beta_1 \beta_2(\beta_2 - \alpha_2) + \alpha_2(\beta_2^2 - \alpha_1^2)) > 0 \quad \text{if} \quad \beta_2 > \alpha_1.$$

To verify $\frac{\partial \lambda}{\partial Q} < 0$, first showing $D(Q) = S(Q) - U(Q) < 0$, where $S(Q) \equiv$ $(\alpha_1 - \alpha_2 + e^{-\gamma Q}(\beta_1 - \beta_2))^2 + 4\beta_1 \beta_2 e^{-\gamma Q}$ and $U(Q) \equiv (\alpha_1 - \alpha_2 + e^{-\gamma Q}(\beta_1 + \beta_2))^2$.

$$D(Q) = 4e^{-\gamma Q}\beta_2(\beta_1 - e^{-\gamma Q}\beta_1 - (\alpha_1 - \alpha_2))$$

$$< 4e^{-\gamma Q}\beta_2\left(\beta_1 - \frac{\beta_1\beta_2 - (\beta_1 - \beta_2)\alpha_2}{\alpha_1\alpha_2}\beta_1 - (\alpha_1 - \alpha_2)\right)$$

$$= 4e^{-\gamma Q}\frac{\beta_2}{\alpha_1\alpha_2}(\beta_1\alpha_2(\alpha_1 - \beta_2) + \beta_1^2(\alpha_2 - \beta_2) + \alpha_1\alpha_2(\alpha_2 - \alpha_1)) < 0. \quad (34)$$

$$\frac{\partial\lambda}{\partial Q} = \frac{1}{4}(S(Q))^{-\frac{1}{2}} \cdot \frac{\partial S(Q)}{\partial Q} + \frac{1}{2}\gamma e^{-\gamma Q}(\beta_1 - \beta_2)$$

$$= \frac{-1}{2}\gamma e^{-\gamma Q}(S(Q))^{-\frac{1}{2}}((\alpha_1 - \alpha_2 + e^{-\gamma Q}(\beta_1 - \beta_2))(\beta_1 - \beta_2)$$

$$+ 2\beta_1\beta_2 - (\beta_1 - \beta_2)(S(Q))^{\frac{1}{2}})$$

$$< \frac{-1}{2}\gamma e^{-\gamma Q}(S(Q))^{-\frac{1}{2}}(e^{-\gamma Q}(\beta_1 - \beta_2)^2 + 2\beta_1\beta_2 - e^{-\gamma Q}(\beta_1 - \beta_2)(\beta_1 + \beta_2))$$

$$= -\gamma e^{-\gamma Q}(S(Q))^{-\frac{1}{2}}\beta_2((1 - e^{-\gamma Q})\beta_1 + e^{-\gamma Q}\beta_2) < 0. \quad (35)$$

Last, we compute the optimal price p^D by solving for it from Eq. (8):

$$E\Pi^D - E\Pi_1^S - E\Pi_2^S - \frac{1}{\gamma}(1 - e^{-\gamma Q}) = K + \frac{\alpha_1}{\gamma}(\ln(\rho) - \ln(\overline{\rho}))$$

$$+ \frac{\beta_1}{\gamma}\left(\frac{1}{\rho} - \frac{1}{\overline{\rho}}\right) - (p - c - \beta_1)Qe^{-\gamma Q}$$

$$- \frac{e^{-\gamma Q}}{\gamma}(\beta_1 - \beta_2)\ln(\overline{\rho})$$

$$- \frac{1}{\gamma}\left(1 - e^{-\gamma Q}\right) \equiv T_1 - (p - c)Qe^{-\gamma Q} \quad (36)$$

$$E\Pi_1^S + E\Pi_2^S = (p - c)\frac{2}{\gamma}(1 - e^{-\gamma Q}) - 2K - (\alpha_1 + \alpha_2)\frac{1}{\gamma}\ln(\rho)$$

$$- (\beta_1 + \beta_2)\frac{1}{\gamma}\left(\frac{1}{\rho} - e^{-\gamma Q}\right) \equiv (p - c)\frac{2}{\gamma}(1 - e^{-\gamma Q}) - T2 \quad (37)$$

$$G(t - p)^2(Qe^{-\gamma Q}) + 2G(t - p)\left(E\Pi^D - E\Pi_1^S - E\Pi_2^S - \frac{1}{\gamma}(1 - e^{-\gamma Q})\right)$$

$$+ E\Pi_1^S + E\Pi_2^S = 0. \quad (38)$$

Let $\bar{t} = t - c - \mu + \delta$,

$$\left(\frac{\bar{t} - (p - c)}{2\delta}\right)^2(Qe^{-\gamma Q}) + \frac{(\bar{t} - (p - c))}{\delta}(T_1 - (p - c)Qe^{-\gamma Q})$$

$$+ (p - c)\frac{2}{\gamma}(1 - e^{-\gamma Q}) - T_2 = 0. \quad (39)$$

$$p^D = c + \frac{-B + \sqrt{B^2 - 4AC}}{2A}, \text{ where } A = Qe^{-\gamma Q}\left(\frac{1}{4\delta^2} + \frac{1}{\delta}\right),$$

$$B = \frac{2}{\gamma}(1 - e^{-\gamma Q}) - \frac{2\bar{t}}{\delta}Qe^{-\gamma Q} - \frac{T_1}{\delta},$$

$$\text{and } C = \frac{\bar{t}^2}{4\delta^2}Qe^{-\gamma Q} + \frac{\bar{t}}{\delta}T_1 - T_2. \tag{40}$$

As Q increases, T_1 increases while T_2 decreases. Thus, both A and C increase, and B decreases. As a result, p^D decreases in Q.

Appendix C: Proof of Proposition 2

We can use Fig. 1 to construct the derivative as the sum of three integrals:

$$\frac{\partial E\Pi^D(q_1^D, q_2^D|p)}{\partial p} = \int_{E_1=0}^{Q}\int_{E_2=0}^{Q-E_1}(E_1 + E_2)dF_2(E_2)dF_1(E_1)$$
$$+ \int_{E_1=0}^{Q}\int_{E_2=Q-E_1}^{\infty}QdF_2(E_2)dF_1(E_1)$$
$$+ \int_{E_1=Q}^{\infty}\int_{E_2=0}^{\infty}QdF_2(E_2)dF_1(E_1) \tag{41}$$

$$\frac{\partial E\Pi^D(q_1^D, q_2^D|p)}{\partial p} = \int_{E_1=0}^{Q}E_1F_2(Q - E_1)dF_1(E_1)$$
$$+ \int_{E_1=0}^{Q}\int_{E_2=0}^{Q-E_1}E_2dF_2(E_2)dF_1(E_1)$$
$$+ Q\int_{E_1=0}^{Q}\overline{F_2}(Q - E_1)dF_1(E_1) + Q\overline{F_1}(Q) \tag{42}$$

$$\frac{\partial E\Pi^D(q_1^D, q_2^D|p)}{\partial p} = \int_{E_1=0}^{Q}\left(E_1F_2(Q - E_1) + Q\overline{F_2}(Q - E_1)\right.$$
$$\left.+ \int_{E_2=0}^{Q-E_1}E_2dF_2(E_2)\right)dF_1(E_1) + Q(1 - F_1(Q)) \tag{43}$$

$$\frac{\partial E\Pi^D(q_1^D, q_2^D|p)}{\partial p} = \int_{E_1=0}^{Q}\left(E_1F_2(Q-E_1)+Q\overline{F_2}(Q-E_1)+(Q-E_1)F_2(Q-E_1)\right.$$
$$\left.- \int_{E_2=0}^{Q-E_1}F_2(E_2)dE_2\right)dF_1(E_1) + Q - QF_1(Q) \tag{44}$$

$$\frac{\partial E\Pi^D(q_1^D, q_2^D|p)}{\partial p} = Q - QF_1(Q) + QF_1(Q)$$
$$- \int_{E_1=0}^{Q}\left(\int_{E_2=0}^{Q-E_1}F_2(E_2)dE_2\right)dF_1(E_1). \tag{45}$$

Using integration by parts and Leibniz' rule on the double integral leads to

$$= Q - \left(F_1(E_1) \int_{E_2=0}^{Q-E_1} F_2(E_2) dE_2 \right) \Bigg|_{E_1=0}^{Q} + \int_{E_1=0}^{Q} F_1(E_1) F_2(Q - E_1) dE_1 \tag{46}$$

$$= Q - \int_{E_1=0}^{Q} F_1(E_1) F_2(Q - E_1) dE_1. \tag{47}$$

Also, $\frac{\partial^2 E\Pi^D(q_1^D, q_2^D|p)}{\partial p^2} = 0$. We can write down the first-order condition on the optimal price:

$$
\frac{\partial E\Pi^D(q_1^D, q_2^D, p)}{\partial p} = 2G(t - p) \cdot (-g(t - p)) \cdot E\Pi^D(q_1^D, q_2^D|p)
$$
$$
+ G^2(t - p) \cdot \frac{\partial E\Pi^D(q_1^D, q_2^D|p)}{\partial p}
$$
$$
+ (1 - 2G(t-p)) \cdot (-g(t-p)) \cdot (E\Pi_1^S(q_1^S|p) + E\Pi_2^S(q_2^S|p))
$$
$$
+ G(t - p) \cdot \overline{G}(t - p) \cdot \left(\frac{\partial E\Pi_1^S(q_1^S|p)}{\partial p} + \frac{\partial E\Pi_2^S(q_2^S|p)}{\partial p} \right)
$$
$$\tag{48}$$

$$
\frac{\partial E\Pi^D(q_1^D, q_2^D, p)}{\partial p} = -2G(t - p) \cdot g(t - p) \cdot E\Pi^D(q_1^D, q_2^D|p)
$$
$$
+ G^2(t - p) \cdot \left(\int_{E_1=0}^{Q} (1 - F_1(E_1) \cdot F_2(Q - E_1)) dE_1 \right)
$$
$$
+ (2G(t - p) - 1) \cdot g(t - p) \cdot (E\Pi_1^S(q_1^S|p) + E\Pi_2^S(q_2^S|p))
$$
$$
+ G(t - p) \cdot \overline{G}(t - p) \cdot \left(\int_{E_1=0}^{Q} \overline{F_1}(E_1) dE_1 \right.
$$
$$
\left. + \int_{E_2=0}^{Q} \overline{F_2}(E_2) dE_2 \right) = 0, \tag{49}
$$

which gives the value of the optimal price p^D. The second-order sufficient condition for p^D is:

$$
\frac{\partial^2 E\Pi^D(q_1^D, q_2^D, p)]}{\partial p^2}
$$
$$
= 2[g'(t - p) \cdot G(t - p) + g^2(t - p)] \cdot E\Pi^D(q_1^D, q_2^D|p)
$$
$$
- 2g(t - p) \cdot G(t - p) \cdot \frac{\partial E\Pi^D(q_1^D, q_2^D|p)}{\partial p}
$$
$$
- [(g'(t - p) \cdot (2G(t - p) - 1) + 2g^2(t - p)] \cdot (E\Pi_1^S(q_1^S|p) + E\Pi_2^S(q_2^S|p))
$$

$$
+ [g(t-p) \cdot (2G(t-p) - 1)] \cdot \left(\frac{\partial E\Pi_1^S(q_1^S|p)}{\partial p} + \frac{\partial E\Pi_2^S(q_2^S|p)}{\partial p} \right)
$$

$$
+ [-g(t-p) \cdot (1 - G(t-p)) + G(t-p) \cdot g(t-p)] \cdot \left(\frac{\partial E\Pi_1^S(q_1^S|p)}{\partial p} + \frac{\partial E\Pi_2^S(q_2^S|p)}{\partial p} \right).
$$
(50)

Thus, p^D must satisfy the second-order condition:

$$
2[g'(t-p^D) \cdot G(t-p^D) + g^2(t-p^D)] \cdot E\Pi^D(q_1^D, q_2^D | p^D)
$$

$$
- 2g(t-p^D) \cdot G(t-p^D) \cdot \left(\int_{E_1=0}^{Q} (1 - F_1(E_1) \cdot F_2(Q - E_1)) dE_1 \right)
$$

$$
- \left[(g'(t-p^D) \cdot (2G(t-p^D) - 1) + 2g^2(t-p^D) \right] \cdot \left(E\Pi_1^S(q_1^S|p^D) + E\Pi_2^S(q_2^S|p^D) \right)
$$

$$
+ \left[4g(t-p^D) \cdot G(t-p^D) - 2g(t-p^D) \right] \cdot \left(\int_{E_1=0}^{Q} \overline{F_1}(E_1) dE_1 + \int_{E_2=0}^{Q} \overline{F_2}(E_2) dE_2 \right) < 0.
$$
(51)

Additionally, we need to impose the following conditions to ensure the expected profit of the storage operator is non-negative:

$$
E\Pi^D \left(q_1^D, q_2^D | p^D \right), \ E\Pi_1^S \left(q_1^S | p^D \right), \ \text{and} \ E\Pi_2^S \left(q_2^S | p^D \right) \geq 0.
$$
(52)

References

1. Baker, E., Nemet, G., Rasmussen, P.: Modeling the costs of carbon capture. In: Zheng, Q.P., Rebennack, S., Pardalos, P.M., Pereira, M.V.F., Iliadis, N.A. (eds.) Handbook of CO_2 in Power Systems Energy Systems Energy Systems, pp. 349–372. Springer, Berlin (2012)
2. Benjaafar, S., Li, Y., Daskin, M.: Carbon footprint and the management of supply chains: insights from simple models. IEEE Trans. Autom. Sci. Eng. **10**(1), 99–116 (2013)
3. Bertsimas, D., Thiele, A.: A data-driven approach to newsvendor problems. Tech. rep., Massachusetts Institute of Technology, Cambridge, MA (2005)
4. Cachon, G.P.: Retail store density and the cost of greenhouse gas emissions. Manag. Sci. (2013)
5. Cai, W., Singham, D., Craparo, E., White, J.: Pricing contracts under uncertainty in a carbon capture and storage framework. Energy Econ. **34**(1), 56–62 (2014)
6. Caro, F., Corbett, C.J., Tan, T., Zuidwijk, R.: Carbon-optimal and carbon-neutral supply chains (2011, working paper)
7. David, J., Herzog, H.: The cost of carbon capture. In: Proceedings of the Fifth International Conference on Greenhouse Gas Control Technologies, Cairns, Australia, pp. 985–990 (2000)
8. Davison, J.: Performance and costs of power plants with capture and storage of CO_2. Energy **32**(7), 1163–1176 (2007)
9. Environmental Protection Agency: 40 CFR Part 60: standards of performance for greenhouse gas emissions from new stationary sources: electrical utility generating units, Washington, D.C. EPA-HQ-OAR-2006-0790 (2013)
10. Environmental Protection Agency: 40 CFR Part 60: carbon pollution emission guidelines for existing stationary sources: electrical utility generating units; Proposed rule, Washington, D.C. EPA-HQ-OAR-2013-0602 (2014)
11. Esposito, R.A., Monroe, L.S., Friedman, J.S.: Deployment models for commercialized carbon capture and storage. Environ. Sci. Technol. **45**(1), 139–146 (2011)

12. Finley, R.J., Frailey, S.M., Leetaru, H.E., Senel, O., Couëslan, M.L., Scott, M.: Early operational experience at a one-million tonne CCS demonstration project, Decatur, Illinois, USA. Energy Procedia **37**, 6149–6155 (2013)
13. Fleten, S.-E., Lien, K., Ljønes, K., Pagès-Bernaus, A., Aaberg, M.: Value chains for carbon storage and enhanced oil recovery: optimal investment under uncertainty. Energy Syst. **1**(4), 457–470 (2010)
14. Global CCS Institute: Global status of large-scale integrated CCS projects, June 2012 update. Global CCS Institute, Canberra (2012)
15. Huang, Y., Rebennack, S., Zheng, Q.P.: Techno-economic analysis and optimization models for carbon capture and storage: a survey. Energy Syst. **4**(4), 315–353 (2013)
16. Huang, Y., Zheng, Q.P., Fan, N., Aminian, K.: Optimal scheduling for enhanced coal bed methane production through CO_2 injection. Appl. Energy **113**, 1475–1483 (2014)
17. Keating, G.N., Middleton, R.S., Viswanathan, H.S., Stauffer, P.H., Pawar, R.J.: How storage uncertainty will drive CCS infrastructure. Energy Procedia **4**, 2393–2400 (2011)
18. Kemp, A.G., Kasim, A.S.: A futuristic least-cost optimisation model of CO_2 transportation and storage in the UK/UK Continental Shelf. Energy Policy **38**, 3652–3667 (2010)
19. Klokk, Ø., Schreiner, P., Pages-Bernaus, A., Tomasgard, A.: Optimizing a CO_2 value chain for the Norwegian Continental Shelf. Energy Policy **38**, 6604–6614 (2010)
20. Middleton, R., Bielicki, J.: A scalable infrastructure model for carbon capture and storage: SimCCS. Energy Policy **37**(3), 1052–1060 (2009)
21. Middleton, R., Kuby, M., Wei, R., Keating, G., Pawar, R.: A dynamic model for optimally phasing in CO_2 capture and storage infrastructure. Environ. Model. Softw. (2012)
22. Rohlfs, W., Madlener, R.: Valuation of CCS-ready coal-fired power plants: a multi-dimensional real options approach. Energy Syst. **2**(3–4), 243–261 (2011)
23. Rubin, E.S., Chen, C., Rao, A.B.: Cost and performance of fossil fuel power plants with CO_2 capture and storage. Energy Policy **35**(9), 4444–4454 (2007)
24. Song, J., Leng, M.: Analysis of the Single-Period Problem Under Carbon Emissions Policies. International Series in Operations Research and Management Science, chap. 13, pp. 297–313. Springer, Berlin (2012)
25. U.S. Environmental Protection Agency: Air Markets Program Data (2013). http://www.ampd.epa.gov